

Design of Robust Decentralized Controllers for Drag-Free Satellite

Lorenzo Pettazzi and Alexander Lanzon and Stephan Theil

Abstract—In this paper the problem of designing a decentralized robust controller for a plant describing a drag-free satellite is addressed. From recent experiences in drag-free control design we first derive an uncertain plant set representative of many drag-free missions with non spherical test masses. A performance requirement is imposed on the absolute acceleration of the test mass along a measurement axis. The main performance requirement is first broken down into requirements on the uncertain closed loop behavior of the system. The fulfillment of this new set of requirements guarantees robust achievement of the overall system goal. Then optimal single-input-single-output controllers are designed that robustly achieve the desired level of performance. The method proposed allows to properly account for the uncertainties in the design plant retaining the decentralized structure of the controller suggested by the peculiar features of the design plant.

I. INTRODUCTION

In recent years space has been considered for high precision physics experiments (see for example LISA Pathfinder [1] and STEP [2]). In all these missions the drag-free satellite concept plays a key role. The drag-free satellite contains a cavity in which a test mass (or proof mass) is let free to fly. The test mass is shielded by the surrounding spacecraft against the disturbances acting on the surface so that its motion is influenced only by the gravitational force and by the small gravitational and electrostatic interaction existing with the spacecraft. Both these contributions show spatial dependence so that a stiffness-like interaction exists between the proof mass and the spacecraft [3]. The accuracy level of the free fall trajectory followed by the test mass depends therefore on the capability of the control system to keep the test mass at the center of the cavity. The free fall requirements are usually specified as acceleration spectral noise densities along a specific axis that is the sensitive axis of the experiment. The control is actuated with high precision continuous thrusters so that the spacecraft is forced to chase the test mass in its purely gravitational motion at least along the sensitive axis. However, for non-spherical proof masses, an electrostatic suspension actuator must be included in order to control the relative attitude of the test mass with respect to the spacecraft.

This work was not supported by any organization.

L. Pettazzi is with Center of Applied Technology and Microgravity, University of Bremen, 28359, Bremen, Germany pettazzi@zarm.uni-bremen.de

A. Lanzon is with the Department of Electrical Engineering, University of Manchester, Manchester, 45435, UK Alexander.Lanzon@manchester.ac.uk

S. Theil is with the DLR Center for Space Systems, Bremen, 28359, Germany Stephan.Theil@dlr.de

The requirements imposed by the scientific goal imply challenging design tasks to be achieved both at a system level and from a control synthesis point of view. From the system design point of view the main objective is to reduce as much as possible the dynamic couplings between the spacecraft and the test mass. For this reason, in many past investigations (see [1] and [2]) it is assumed that the couplings among the different degrees of freedom are highly reduced. This allows to tackle the control design procedure as a synthesis of a set of single-input-single-output (SISO) controllers completely ignoring the coupling effects. In all these cases no structured uncertainty is considered in the design plant so that the achievement of the top level performance requirement of the whole system in the presence of perturbations must be checked *a posteriori*.

In this paper the problem of designing a decentralized robust controller for a plant describing a two-degrees-of-freedom drag-free satellite is addressed in a more systematic way. A design plant representative of the most modern drag-free satellites ([1], [4]) is first defined. Then a two stage design technique is proposed. In the first phase the measurement relation is exploited to derive bounds on the individual closed loop responses, that, when satisfied, guarantee the robust performance of the overall system. In the second phase, a recently developed control design technique [5] based on the mixed structured singular value is used to synthesize SISO controllers that robustly achieve the performance specified by the individual bounds.

The proposed methodology allows for the direct design of a decentralized controller that automatically achieves robust performance and, on the other hand, it helps to assess if the overall system goal is achievable by independent controller designs.

A. Notation

Let $\overline{\mathbb{R}}_+$ denote the non negative real numbers, $\overline{\mathbb{C}}_+$ denote the closed right half complex plane and $\mathbb{C}^{m \times n}$ denote complex matrices of dimension $m \times n$. The maximum singular value of a matrix $A \in \mathbb{C}^{m \times n}$ is denoted by $\overline{\sigma}(A)$. A^T (resp. A^*) is the transpose (resp. complex conjugate transpose) of $A \in \mathbb{C}^{m \times n}$ and $\|A\|_F$ denotes the Frobenius norm of the matrix A . The $k \times k$ identity matrix and zero matrix are denoted by I_k , and O_k respectively and \otimes denotes the Kronecker product. A real rational matrix function $\Gamma(s)$ of a complex variable s is such that $\Gamma(s) \in \mathcal{RH}_\infty$ if it is bounded and analytic in the open complex right half plane. The $\|\cdot\|_\infty$ norm of a $m \times n$ matrix function $\Gamma(s)$ is defined by $\|\Gamma\|_\infty := \sup_{\omega} \overline{\sigma}(\Gamma(j\omega))$. Finally, $\text{diag}_{i=1}^N(A_i)$ with $A_i \in \mathbb{C}^{m_i \times n_i}$, $i = 1, \dots, N$ denotes the

$\sum_i m_i \times \sum_i n_i$ block diagonal complex matrix composed of A_i , $i = 1, \dots, N$.

II. PLANT MODEL

The drag-free satellite can be divided in two different subsystems, the spacecraft and the experiment on board. The experiment includes a cavity (or housing) that contains a partially free flying cubic proof mass. Position and attitude of the test mass with respect to the spacecraft are measured by means of an electrostatic sensor. In the direction of the sensitive axis high precision Field Emission Electric Propulsion (FEEP) thrusters are used to control the position of the satellite such that the proof mass remains in the center of the cavity. A suspension actuation system is required to align the test mass attitude to the one of the satellite (see [3] and references therein). The design of the attitude control for the spacecraft is assumed and is not described in the present paper.

In the remainder of this section the linearized equations describing the motion of the test mass with respect to the spacecraft are derived. In particular, the simplified model in this paper considers only the displacement along the spacecraft x body axis and the rotation ϕ around the spacecraft z body axis. However, the control design technique here developed is general and can be easily applied to more complex dynamic models. The set of linearized equations describing the relative motion of the test mass with respect to the spacecraft is [4]:

$$\ddot{q} = M_q^{-1} [f_e + f_{exp} + f_h + M_u \ddot{q}_{SC}] \quad (1)$$

where $q = [x, \phi]^T$, $M_q = \text{diag}(m_{TM}, I_{TM})$ represents the proof mass generalized mass matrix (mass plus inertia), M_u is the sensitivity of the test mass dynamics to the spacecraft linear (\ddot{x}_{SC}) and angular ($\ddot{\phi}_{SC}$) acceleration, expressed in the vector \ddot{q}_{SC} . The generalized forces (forces and torques) acting on the test mass are divided in three contributions f_e , f_{exp} and f_h . A brief description of the three terms is presented in the following:

- f_e are the external generalized forces acting on the test mass.
- f_{exp} are the gravitational generalized forces acting between test mass and the experiment.
- f_h are the the electrostatic generalized forces acting between electrode housing and the test mass.

Both f_{exp} and f_h show spatial dependence so that it is convenient to represent them by means of a series expansion:

$$f_h = f_{h_0} + f_{sus} + K_h q \quad (2)$$

$$f_{exp} = f_{exp_0} + K_{exp} q \quad (3)$$

where f_{sus} are the electrostatic suspension generalized forces acting on the test mass and $K_{exp} := \partial f_{ext} / \partial q$ and $K_h := \partial f_h / \partial q$ are the corresponding stiffness matrices. Moreover, a direct cross-talk is included in the electrostatic actuation. The relation between the commanded suspension forces F_{sus} and the real ones f_{sus} can be expressed by

$$f_{sus} = (I + H_{IS}) F_{sus}$$

where H_{IS} is the actuation cross-talk matrix.

The approximated linearized equation of motion of the spacecraft is

$$\ddot{q}_{SC} = M_{SC}^{-1} [f_{dist} + f_{DF}] \quad (4)$$

where M_{SC} is the spacecraft generalized mass matrix and f_{dist} is the external disturbance acting on the spacecraft. Assuming that the satellite is placed in a low disturbance environment, for example in the Earth-Sun Lagrangian point [1], the main contribution to the disturbance force acting on the satellite is solar radiation drag.

TABLE I
NUMERICAL DATA OF THE DRAG-FREE SATELLITE

Parameter		Numerical Value	
m_{SC}		500 kg	
I_{SC}		500 kg · m ²	
m_{TM}		1 kg	
I_{TM}		6 · 10 ⁻⁴ kg · m ²	
$K :=$	K_{xx} $K_{x\phi}$	2	0.003
	$K_{\phi x}$ $K_{\phi\phi}$	0.006	0.004
		· 10 ⁻⁶ $\frac{N}{m}$	
$H_{IS} :=$	0 h_{IS}	0	0.5
	h_{IS} 0	0.5	0

f_{DF} contains the force and torque acting on the spacecraft due to the drag-free control. This action is provided by means of FEEP thrusters, modeled here as a first order system with a characteristic rise time of approximately 0.3 sec. The selected rise time takes into account the delays introduced by the electronic devices driving the thrusting actuators. Substituting (2), (3) and (4) into (1) yields the following expression:

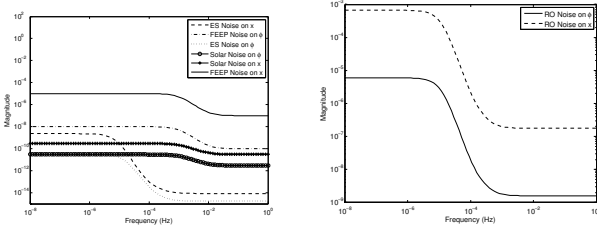
$$\ddot{q} = M_q^{-1} \{Kq + f_{sus} + f_{TM} + (M_u M_{SC}^{-1})(f_{dist} + f_{DF})\} \quad (5)$$

where $K = K_{exp} + K_h$ and $f_{TM} = f_{h_0} + f_{exp_0} + f_e$ is the disturbance force directly acting on the proof mass (dominated by the electrostatic interaction). The numerical values of the physical characteristics of the system are displayed in Table I whereas the frequency content of the disturbance forces are displayed in Figure 1 together with the measurement noise associated to the electrostatic sensor. They are all consistent with those given in [1] describing a similar system.

In order to translate the science objective into controller requirements the measurement equation must be derived. In the example considered in this paper, a performance requirement is imposed on the residual absolute acceleration along the x axis. This can be expressed as a function of the noises on the coordinates x and ϕ and of the suspension actuation and disturbance forces acting upon the test mass as:

$$y = m_{TM}^{-1} [f_{TM_x} + h_{IS} F_{sus\phi} + K_{xx} x + K_{x\phi} \phi]. \quad (6)$$

Uncertainty is introduced in the plant model to take into account the unknown behavior of the system. In particular, the force interaction between the spacecraft and the test mass is difficult to estimate and, therefore, an uncertainty of $\pm 50\%$ with respect to the nominal value listed in Table I



(a) Input disturbances weights. (b) Read out disturbances weights. Units for disturbance on x is $\text{N}/\sqrt{(\text{Hz})}$, on ϕ is $\text{Nm}/\sqrt{(\text{Hz})}$. $\text{m}/\sqrt{(\text{Hz})}$, on ϕ is $\text{rad}/\sqrt{(\text{Hz})}$.

Fig. 1. Input and read out disturbance weights.

is considered on both K and H_{IS} . Moreover, an uncertainty of $\pm 5\%$ on the scale factor and an uncertainty of $\pm 50\%$ on the FEEP characteristic time takes into account the undetermined behavior of the thruster.

III. DERIVATION OF SPECIFICATIONS FOR DECENTRALIZED CONTROL DESIGN

In this work the control design will be considered successful if the residual absolute acceleration acting on the test mass along the x direction is kept below

$$\mathcal{A}_y^{1/2} \leq 2 \cdot 10^{-14} \left[1 + \left(\frac{f}{3\text{mHz}} \right)^2 \right] \frac{\text{m}}{\text{s}^2} \frac{1}{\sqrt{\text{Hz}}} \quad (7)$$

in the measurement bandwidth (MBW) $f \in [1, 30]$ mHz in the presence of uncertainty as defined in the previous section. This requirement represents the technological goal of missions currently under development (see [1]) and therefore it will be taken here as reference. Moreover, a decentralized controller structure is assumed in this work where the test mass x position is fed back by means of the thruster actuation (drag-free controller K_{DF}) and the attitude error is fed back by means of the suspension actuation (suspension controller K_{SUS}). This situation is encountered when the requirement of (7) must be satisfied together with a requirement on the orientation of the spacecraft. Being the main science objective to reduce the residual action on the test mass along the x direction, the choice to control the test mass x position with the thruster is highly recommended.

The constraint imposed on the controller structure does not allow, in principle, the application of the classical μ -synthesis technique ($D-K$ iteration) to the MIMO system. An attractive alternative solution is to break down the nearly diagonal uncertain plant into two different SISO plants neglecting in the definition of the uncertain plant set the off diagonal elements of the stiffness matrix. This approximation is justified by the fact that, as can be seen from the numerical values listed in Table I, the stiffness matrix is highly diagonal dominant. The resulting simplified plant is therefore the one shown in Fig. 2 where we define

$$\Gamma_{DF} = \frac{1}{s^2 - \frac{K_{xx}}{m_{TM}}} \Gamma_{FEEP}$$

$$\Gamma_{SUS} = \frac{1}{s^2 - \frac{K_{\phi\phi}}{I_{TM}}}$$

Note that, h_{IS} together with the off-diagonal elements of K appear also in the measurement equation. Therefore, an uncertainty on these parameters may still be critical for the achievement of the top level requirement and must be properly accounted for.

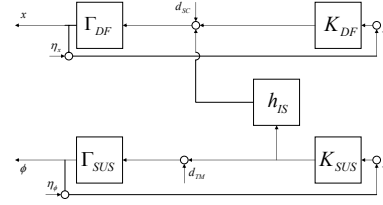


Fig. 2. Decoupled MIMO block diagram of the drag-free satellite system.

To this end, we write the closed loop expression of both the two individual loops and we substitute it into (6) to obtain an approximation of the closed loop measurement equation

$$y(s) \approx m_{TM}^{-1} \{ f_{TM_x} + K_{xx} [S_{DF} \Gamma_{DF} d_{SC} - T_{DF} \eta_x] + K_{x\phi} [S_{SUS} \Gamma_{SUS} d_{TM} - T_{SUS} \eta_\phi] \} + h_{IS} (1 + K_{xx} m_{TM}^{-1} S_{DF} \Gamma_{DF}) [-T_{SUS} d_{TM} - T_{SUS} / \Gamma_{SUS} \eta_\phi] \quad (8)$$

where the standard notation is used for the sensitivity and complementary sensitivity functions both for the drag-free and the suspension loops. Note that the coupling between the suspension and drag-free loops is taken into account in the derivation of (8). In this paper the measurement equation in (8) is used to break down the requirements in (7) into independent requirements on the closed loop behavior of the drag-free and suspension loops. The fulfillment of these requirements is a sufficient condition of robust performance of the overall system. Then a novel control design technique (see [5]) is used to synthesize SISO controllers that robustly achieve the individual requirements. The synthesis algorithm involves the iterative solution of an optimization problem aimed at maximizing the size of the performance weights, used to shape the design of the individual controllers, to achieve desired specifications. This optimization is restricted by the constraint that there exists an internally stabilizing controller that achieves robust performance with respect to the maximized weights. The designer is only required to specify the plant uncertain set and some frequency dependent functions, dubbed optimization directionalities, that reflect, in a qualitative way, the desired performance requirements over all frequency. The specification of the optimization directionality functions is easier than the direct design of the performance weights and can be easily derived by the information about the way the different exogenous disturbances enter in the performance cost in (8).

IV. CONTROL SYNTHESIS TECHNIQUE

In this work the optimization based synthesis technique introduced in [5] is used to design the suspension and drag-free controllers. In the following, for the sake of completeness, a brief description of the synthesis method is given.

The interested reader can find a more detailed description in the referenced paper.

First of all let us define a set of uncertain matrices with a given structure:

$$\begin{aligned} \Delta := \{ & \Delta = \text{diag}[I_{n_1} \otimes \Delta_1, \dots, I_{n_g} \otimes \Delta_g, I_{n_{g+1}} \otimes \Delta_{g+1}, \\ & \dots, I_{n_{g+d}} \otimes \Delta_{g+d}] : \Delta_i = \Delta_i^T \in \mathbb{R}^{k_i \times k_i} \forall i \in \{1, \dots, g\} \\ & \text{and } \Delta_i \in \mathbb{C}^{k_i \times k_i} \forall i \in \{g+1, \dots, g+d\} \}. \end{aligned} \quad (9)$$

where $\sum_{i=1}^{g+d} n_i k_i = r$. A set of uncertain stable transfer function matrices with structure Δ can be then defined as:

$$\Pi_\Delta := \{\Delta(s) \in \mathcal{RH}_\infty : \Delta(s_0) \in \Delta \forall s_0 \in \overline{\mathbb{C}}_+, \|\Delta\|_\infty \leq 1\}. \quad (10)$$

Most linear time invariant closed loop systems subject to perturbations can be redrawn into the form depicted in Fig. 3(a), where $\Gamma(s)$ is the known part of the plant partitioned consequently with the interconnection. In Fig. 3(a), $\Delta(s) \in \Pi_\Delta$ represents a stable perturbation with r inputs and r outputs whereas $K(s)$ is an internally stabilizing controller with p inputs and q outputs. The system is subject to the exogenous disturbances d and the control objective is measured in terms of the error signals e . The required performances of the closed loop system are included in the design by means of the diagonal frequency dependent performance weight $W \in \mathcal{W} := \{\text{diag}_{i=1}^n [w_i] : w_i \in \mathcal{RH}_\infty\}$ with $i = 1, \dots, n$. The system achieves robust performance in the presence of uncertainty if

$$\|W \mathcal{F}_u(\mathcal{F}_l(G, K), \Delta)\|_\infty < 1 \quad (11)$$

where $\mathcal{F}_u(\cdot, \cdot)$ and $\mathcal{F}_l(\cdot, \cdot)$ are the lower and upper linear fractional transformations (see [6] for further details). The condition in (11) can be rewritten in terms of the supremum of the structured singular value (denoted by μ [6])

$$\sup_{\omega} \mu_{\Delta_T} \left[\begin{pmatrix} I & 0 \\ 0 & W(j\omega) \end{pmatrix} \mathcal{F}_l(\Gamma(j\omega), K(j\omega)) \right] < 1 \quad (12)$$

where $\Delta_T := \{\text{diag}(\Delta, \Delta_p) : \Delta \in \Delta, \Delta_p \in \mathbb{C}^{m \times n}\}$ denotes the total uncertainty structure with respect to which the structured singular value is computed (see Fig. 3(b)). However, for common applications upper and lower bounds of μ_Δ are computed. A classical μ design problem with given performance and robustness specifications involves the search for a controller that minimizes the left hand side of (12). In other cases it may be desirable to maximize the performance of the system subject to the condition in (12). The control synthesis problem may be then reformulated as in [7]:

$$\min_{\mathcal{K}} \sup_{\omega} \mu_{\Delta_T} \left[\begin{pmatrix} I & 0 \\ 0 & W(j\omega) \end{pmatrix} \mathcal{F}_l(\Gamma(j\omega), K(j\omega)) \right] < 1 \quad (13)$$

where $J(W)$ is an objective function that captures the performance preferences of the design and \mathcal{K} is the set of all internally stabilizing controllers for the system $\mathcal{F}_l(\Gamma, K)$. In this case the optimization algorithm simultaneously synthesizes the controller and the weighting functions to maximize

the closed loop performance of the system in some sense. A pointwise in frequency solution of the optimization problem in (13) is proposed in [7] in the case of purely complex structured uncertainty. In the following a brief description of the synthesis method capable to handle both parametric and complex uncertainties is given.

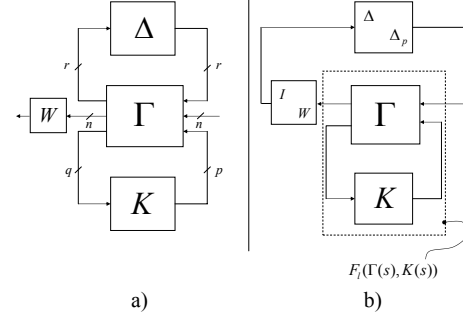


Fig. 3. Generalized block interconnection for synthesis and analysis.

A. Objective Function Definition

The objective function in (13) must be able to capture the performance preferences of the design that in common practice are reflected as gain requirements on the closed loop transfer functions. These gain requirements are usually handled by penalizing each output of the closed loop system with a weight, $w_i(j\omega)$, whose magnitude reflects the inverse of the desired specification bound. The objective function in (13) shall then represent a cumulative measure across frequency that reflects qualitatively the desired inverse performance weights shape.

Following the work in [7], let $[\omega_L, \omega_H]$ be a synthesis frequency range and $v_i(j\omega)$ be n given stable minimum phase transfer functions. Let us define

$$J(W) = \frac{1}{\int_{\log \omega_L}^{\log \omega_H} \sum_{i=1}^n \frac{1}{|w_i(j\omega)/v_i(j\omega)|^2} d(\log \omega)}. \quad (14)$$

The direction of steepest ascent in maximizing the function in (14) over any one weight $w_i(j\omega)$ at any one frequency ω in the frequency interval $[\omega_L, \omega_H]$ corresponds to the smallest ratio $|w_i(j\omega)/v_i(j\omega)|$. Consequently, the functions $v_i(j\omega)$ are called optimization directionalities because they can be specified so that they qualitatively direct the maximization where desired. Therefore $|v_i(j\omega)|$ should be set at a large value (resp. small) at frequencies and in channel directions where the magnitude of the performance weight $w_i(j\omega)$ is required to be large (resp. small) in order to capture the desired performance objectives. Defining an optimization directionality matrix as $\Upsilon(j\omega) := \text{diag}(v_1(j\omega), \dots, v_n(j\omega))$, then (similar to [7]) the cost function in (13) can be defined as:

$$J(W) = \frac{1}{\|\Upsilon W^{-1}\|_{[\omega_L, \omega_H]}^2},$$

where $\|X\|_{[\omega_L, \omega_H]} := \sqrt{\int_{\log \omega_L}^{\log \omega_H} \|X(j\omega)\|_F^2 d(\log \omega)}$. Note that only the argument of the optimization is of interest.

Therefore the maximization of the cost can be replaced by the minimization of the reciprocal of $J(W)$ as will be seen in the next subsection.

B. Search Space Definition

In every optimization problem a crucial issue is the definition of the search space. First of all, since $\mu_\Delta(M) = \mu_\Delta(M^T)$, the optimization problem in (13) can be equivalently rewritten in terms of the dual system

$$\min_{W \in \mathcal{W}} \|\Upsilon W^{-1}\|_{[\omega_L, \omega_H]}^2 \quad \text{subject to} \quad (15)$$

$$\min_{K \in \mathcal{K}} \sup_{\omega} \mu_{\Delta_T} [\mathcal{F}_l(\Gamma, K)(j\omega)^T \text{diag}[I_r, W(j\omega)]] < 1$$

so that the inverses of the performance weights will appear in subsequent manipulations independently to form a convex constraint.

Now, in order to define an efficient solution algorithm, the robust performance constraint written in terms of μ_{Δ_T} will be replaced with a convex upper bound. Such an upper bound involves the definition of matrix scalings G and D allowed to vary in sets \mathcal{D} and \mathcal{G} that depend on the structure of the perturbation matrix Δ (see [6] for further details). The following lemma from [6] defines an upper bound on the structured singular value:

Lemma 1: [6] Let $M \in \mathbb{C}^{r \times r}$ and $\Delta \in \Delta$. Then

$$\mu_\Delta(M) \leq \inf_{D \in \mathcal{D}, G \in \mathcal{G}} \min_{\beta} \{\beta : M^*DM + j(GM - M^*G) - \beta^2 D \leq 0\} \quad (16)$$

This result can be reformulated in a more convenient way exploiting the result from the following Lemma

Lemma 2: [5] Given a complex matrix $M \in \mathbb{C}^{r \times r}$, $D \in \mathcal{D}$, $G \in \mathcal{G}$, $\beta > 0$ and $\gamma \in [0, 1]$, then

$$\bar{\sigma} \left(\left(\frac{DMD^{-1}}{\beta} - jG \right) (I + G^2)^{-\frac{1}{2}} \right) \leq \gamma \quad (17)$$

if and only if

$$\Omega(M, \hat{G}, \hat{D}, \beta, \gamma) := \begin{bmatrix} M^* \hat{D} M + j(\hat{G} M - M^* \hat{G}) - (\beta \gamma)^2 \hat{D} & \sqrt{1 - \gamma^2} \hat{G} \\ \sqrt{1 - \gamma^2} \hat{G} & -\hat{D} \end{bmatrix} \leq 0 \quad (18)$$

where $\hat{D} = D^* D \in \mathcal{D}$ and $\hat{G} = \beta D^* G D \in \mathcal{G}$.

By virtue of Lemma 2 an equivalent reformulation of the upper bound in (16) is:

$$\Omega(M, G, D, \beta, 1) \leq 0. \quad (19)$$

Note that by adding the fictitious uncertainty block $\Delta_p \in \mathbb{C}^{n \times n}$ to handle robust performance problems, the scaling matrices associated to the augmented uncertainty structure Δ_T are $\text{diag}[D, I_n]$, $D \in \mathcal{D}$ and $\text{diag}[G, 0_n]$, $G \in \mathcal{G}$ where the last entry in the D -scales has been normalized to unity. The following lemma provides an equivalent reformulation of the upper bound on $\mu_{\Delta_T} [\mathcal{F}_l(\Gamma, K)(j\omega)^T \text{diag}[I_r, W(j\omega)]]$.

Lemma 3: [5] Given a closed loop system $\mathcal{F}_l(\Gamma, K) \in \mathcal{RH}_\infty$ and performance weights $W \in \mathcal{W}$. Then, $\forall \omega \exists D_\omega \in \mathcal{D}, G_\omega \in \mathcal{G}, \gamma_\omega \in [0, 1]$ and $\beta_\omega > 0$ such that

$$\Omega(\mathcal{F}_l(\Gamma, K)(j\omega)^T \text{diag}[I_r, W(j\omega)], \text{diag}[G_\omega, 0_n], \text{diag}[D_\omega, I_n], \beta_\omega, \gamma_\omega) \leq 0 \quad (20)$$

if and only if $\forall \omega \exists D_\omega \in \mathcal{D}, G_\omega \in \mathcal{G}, \gamma_\omega \in [0, 1]$ and $\beta_\omega > 0$ such that

$$\Omega(\mathcal{F}_l(\Gamma, K)(j\omega)^T, \text{diag}[G_\omega, 0_n], \text{diag}[D_\omega, I_n], \beta_\omega, \gamma_\omega) \leq \text{diag}[0_r, (\beta_\omega \gamma_\omega)^2 (W_\omega - I_n), 0_{r+n}]$$

where $W_\omega = [W(j\omega)^* W(j\omega)]^{-1}$.

With the result from lemma 3, and using the aforementioned upper bound of μ , the optimization problem in (13) is replaced by the following one:

$$\min_{W \in \mathcal{W}} \|\Upsilon W^{-1}\|_{[\omega_L, \omega_H]}^2 \quad \text{such that} \quad (21)$$

$$\forall \omega \exists D_\omega \in \mathcal{D}, G_\omega \in \mathcal{G} \text{ and } \beta_\omega \in (0, 1) \text{ satisfying}$$

$$\Omega(\mathcal{F}_l(\Gamma, K)(j\omega)^T, \text{diag}[G_\omega, 0_n], \text{diag}[D_\omega, I_n], \beta_\omega, 1) \leq \text{diag}[0_r, \beta_\omega^2 (W_\omega - I_n), 0_{r+n}].$$

When K is held fixed, the search space in (21) can be characterized by a set of LMI constraints, uncoupled at each ω , and simultaneously quasi-convex in D_ω , G_ω , W_ω and β_ω . This fact is used to propose an iterative solution algorithm that can be divided in two phases. In the first one the controller K is fixed and we find the biggest possible performance weights and scalings given a fixed level of uncertainty and a given controller K . In the second phase the scalings and the weights are absorbed in the generalized plant and an optimal controller is designed via \mathcal{H}_∞ synthesis techniques. Further details on the solution algorithm are given in [5].

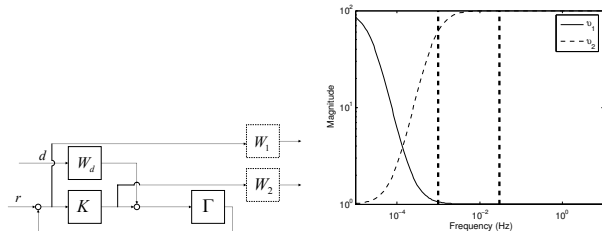
V. DESIGN RESULTS

The synthesis technique outlined in the previous section is exploited to design the drag-free and suspension SISO controllers. First the top level requirement in (7) is broken down into specifications on the drag-free and suspension loops respectively. Such specifications, given in the MBW, are shown in Table II and are derived from the closed loop measurement relation in (8) in which we substitute the worst case combination of parameters. Then the synthesis technique outlined in section IV is used to separately design the two SISO controllers. In this paper, for the sake of conciseness, only the design of the suspension controller is described in detail. However, as mentioned in [1], this is the axis that presents the greatest challenges from the control design point of view.

The inputs to the synthesis algorithm for the suspension controller design are shown in Fig. 4. The performance weights W_1 and W_2 are automatically defined by the synthesis algorithm to shape S and $T\Gamma^{-1}$. In particular, the high magnitude of $v_1(j\omega)$ at low frequencies (below 1mHz) implies that the optimization algorithm should maximize W_1 at low

TABLE II
SPECIFICATIONS ON THE INDIVIDUAL LOOPS

Variable	Specification in the MBW
x	$3.05 \cdot 10^{-9} \left[1 + \left(\frac{f}{3\text{mHz}} \right)^2 \right] \frac{\text{m}}{\sqrt{\text{Hz}}}$
ϕ	$2.33 \cdot 10^{-6} \left[1 + \left(\frac{f}{3\text{mHz}} \right)^2 \right] \frac{\text{rad}}{\sqrt{\text{Hz}}}$
u_{ES}	$2.33 \cdot 10^{-11} \left[1 + \left(\frac{f}{3\text{mHz}} \right)^2 \right] \frac{\text{rad}}{\text{s}^2 \sqrt{\text{Hz}}}$



(a) Suspension controller design (b) Optimization directionalities. set-up.

Fig. 4. Input to the synthesis algorithm for suspension controller design.

frequencies. This is necessary to attenuate the disturbances in input to the suspension loop. On the other hand the high magnitude of $v_2(j\omega)$ at high frequencies (above 1mHz) states that the optimization problem should maximize as much as possible W_2 in the MBW. This will limit the effect of the inertial sensor readout noise on the suspension control force that couples directly with the measurement equation. The optimization problem in (21) is approximated through gridding on a frequency grid of 150 points in the range between $[10^{-5}\text{Hz}, 10^1\text{Hz}]$. The resulting controller is, after proper order reduction, of 4th order. The algorithm converges after 5 iterations. In Fig. 5 the pointwise in frequency magnitudes of the inverses W_1 and W_2 in output to the synthesis algorithm are shown together with the nominal closed loop transfer functions S and $T\Gamma^{-1}$. The magnitude plot of each uncertain closed loop sensitivity function falls below the corresponding weight since robust performance is guaranteed. In Fig. 6 the response of the system from input disturbance and read out noise to control signal, obtained closing the suspension loop shown in Fig. 2 with the designed controller is displayed. In this figure it is possible to see that the worst case transfer function from read out noise to actuation signal (line with “bullet” markers) clears the performance requirements.

As a final remark note that the fully coupled closed loop uncertain system achieves robust performance being the maximum value of μ over frequency 0.85.

VI. CONCLUSION

This work addresses the problem of the design of a robustly performing decentralized controller for a high accuracy drag-free satellite with cubic test mass. First an uncertain design plant set representative of the most modern drag-free satellites missions has been defined. The measurement equation has been exploited to perform a worst case performance breakdown to derive requirements on the closed

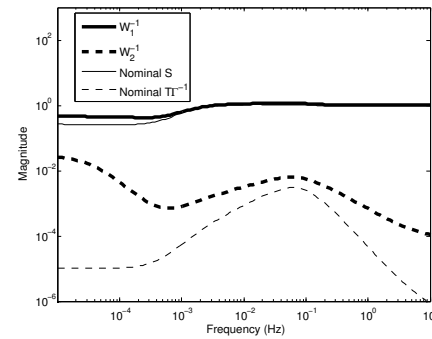


Fig. 5. S and $T\Gamma^{-1}$ plots and corresponding performance weights in output to the synthesis algorithm.

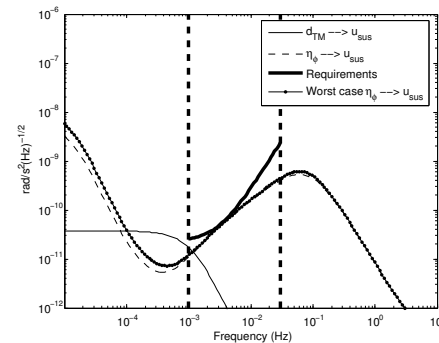


Fig. 6. Closed loop response of the nominal suspension SISO system in terms of suspension control signal.

loop transfer functions of the individual loops. A recently developed iterative algorithm that performs an optimized trade off between achievable performance and limitations due to uncertainty or plant dynamics, has been then considered to independently design the controller of each loop. The resulting design technique has shown to be easy and allows to properly account for the uncertainty appearing in both the design plant and in the measurement equation while retaining the decentralized structure of the controller.

REFERENCES

- [1] P. Gath, W. Fichter, M. Kersten, and A. Schleicher, “Drag free and attitude control system design for the LISA pathfinder mission,” in *AIAA Guidance, Navigation, and Control Conference and Exhibit*, Providence, Rhode Island, U.S.A., 2004.
- [2] Y. Jafray, “Drag-free Control for MiniSTEP,” *Classical Quantum Gravity*, no. 13, 1996.
- [3] W. Fichter, A. Schleicher, S. Bennani, and S. Wu, “Closed Loop Performance and Limitations of the LISA Pathfinder Drag-Free Control System,” in *AIAA Guidance and Navigation and Control Conference and Exhibit*, Hilton Head, South Carolina, August 2007.
- [4] D. Bortoluzzi, M. Da Lio, R. Dolesi, W. Weber, and S. Vitale, “The LISA technology package dynamics and control,” *Classical Quantum Gravity*, vol. 20, pp. 227–238, 2003.
- [5] L. Pettazzi and A. Lanzon, “Systematic Design of Optimal Performance Weight and Controller in mixed- μ Synthesis,” in *8th IFAC World Congress*, Seoul, Korea, 2008.
- [6] K. Zhou and J. Doyle, *Essentials of Robust Control*. Prentice Hall, 1999.
- [7] A. Lanzon, “Pointwise in frequency weight optimization in μ -synthesis,” *International Journal of Robust and Nonlinear Control*, vol. 15, pp. 171–199, 2005.